Performance analysis of space-shift keying over negative-exponential and log-normal FSO channels

Mohamed Abaza[1,*], Raed Mesleh[2], Ali Mansour[3], and el-Hadi Aggoune[1]

[1]*Sensor Networks and Cellular Systems (SNCS) Research Center, University of Tabuk, 71491 Tabuk, Saudi Arabia*
[2]*Electrical Engineering Department, University of Tabuk, P.O. Box 741, 71491 Tabuk, Saudi Arabia*
[3]*Lab STICC, ENSTA Bretagne, 2 Rue François Verny, 29806 Brest Cedex 9, France*
**Corresponding author: mabaza.sncs@ut.edu.sa*

Received December 29, 2014; accepted March 26, 2015; posted online April 29, 2015

The average bit-error rate (ABER) performance of free-space optical (FSO) communication links is investigated for space-shift keying (SSK) over log-normal and negative-exponential atmospheric turbulence channels. SSK is compared with repetition codes and a single-input single-output system using multiple pulse amplitude modulations. Simulation results show that the signal-to-noise ratio gain of SSK largely increases with greater spectral efficiencies and/or higher turbulence effects. A tight bound for ABER is derived based on an exact moment generation function (MGF) for negative-exponential channel and an approximate MGF for log-normal channel. Finally, extensive Monte Carlo simulations are run to validate the analytical analysis.

OCIS codes: 010.1300, 010.1330, 060.4510.
doi: 10.3788/COL201513.051001.

Free-space optical (FSO) communication is a leading subject that has been in the forefront of both research and commercial activities over the past years. Such attention is driven by the promise of high data rate, license-free operation, and reduced cost as well as being eco-friendly as compared to alternative communication means that are greatly suffering from, among other things, congestion[1,2]. However, several challenges, such as turbulence[3], pointing error losses[4], attenuation from weather elements[5], and challenges such as installation and maintenance costs are yet to be addressed. Among these challenges are atmospheric turbulence which causes scintillation of the laser beam due to temperature and pressure variations that have been shown to adversely affect FSO systems[5]. FSO turbulence is modeled by statistical models that fit experimental results[6], including log-normal for weak–moderate[5], gamma–gamma (G–G) for moderate–strong[4], and negative-exponential[7] for strong (saturated) turbulence regimes.

To reduce the impact of atmospheric turbulence effects, some potential solutions such as channel coding[8] and the use of multiple apertures at the receiver and multiple beams at the transmitter[9] have been proposed. To this end, different multiple-input multiple-output (MIMO) techniques have been proposed for FSO systems. Specifically, spatial modulation (SM)[10] MIMO system for indoor optical wireless communication has been studied in Ref. [11]. In SM, a group of data bits modulate a symbol from certain constellation diagram and another group activates one of the transmitter beams. Detailed information about SM and space-shift keying (SSK) systems can be found in Ref. [12]. A line-of-sight (LOS) indoor optical wireless communication system using SM is proposed in Ref. [13]. Results revealed that SM outperforms its counterpart repetition codes (RCs) system with multiple pulse amplitude modulation (MPAM) for spectral efficiencies larger than 4 bits/s/Hz. In Ref. [14], spatial pulse position amplitude modulation (SPPAM) is proposed for FSO links. It is shown that SPPAM outperforms SSK for spectral efficiencies of 2 bits/s/Hz or less.

SSK is a special case of SM where no data symbol is transmitted and transmitted information is conveyed through the spatial position of the active transmitter. Another study conducted in Ref. [15] shows that on–off keying (OOK) RC outperforms orthogonal space–time block codes (OSTBCs), spatial multiplexing (SMux), and SSK for FSO communications using intensity modulation (IM) with direct detection (DD) over G–G channels. However, these results are given only for a spectral efficiency of 1 bit/s/Hz.

The main contributions of this letter are: (i) SSK is proposed as a high-spectral-efficiency modulation technique for FSO links; (ii) exact moment generation function (MGF) and approximate MGF of the absolute difference of negative-exponential and log-normal channels for SSK are derived, respectively; (iii) tight bounds bit-error rate (BER) are obtained based on the derived MGFs and validated using Monte Carlo (MC) simulations; (iv) performance comparison with state-of-the-art RC MPAM for IM/DD FSO communication system is presented and results show that SSK outperforms RC MPAM for spectral efficiencies of 4 bits/s/Hz or larger over moderate–strong atmospheric turbulence channels.

A SSK system with N_t transmitters and N_r receivers is illustrated in Fig. 1. A value of $\log_2(N_t)$ bits are transmitted at each particular time instant and are mapped to the

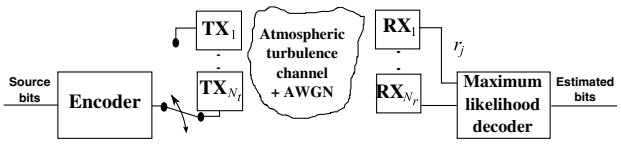

Fig. 1. Synoptic diagram of the proposed model.

spatial location, k, of one of the existing N_t transmitters. Thereby, only one transmitter becomes active at a particular time instant, while other transmitters remain silent[10]. The transmitted light propagates over a negative-exponential channel for a strong turbulence or a log-normal channel for a moderate turbulence. Furthermore, it is assumed that the received signal suffers from shot, thermal, and dark noise. The shot noise is assumed to dominate other noise sources[16] and it can be modeled as an additive white Gaussian noise (AWGN).

The received signal vector $\mathbf{r}$ is given by

$$\mathbf{r} = \eta \mathbf{H} + \mathbf{n}, \tag{1}$$

where $\mathbf{r} \in \mathbb{C}^{N_r \times 1}$ with received signal at each branch, r_j, η is the optical-to-electrical conversion coefficient, $\mathbf{H} \in \mathbb{C}^{N_r \times N_t}$ is the channel irradiance matrix with channel irradiance entries, $h_{jk} \geq 0$ denotes the channel irradiance between the active transmitter $k = 2^p$; $1 \leq p \leq \log_2(N_t)$ and receiver $j = 1, ..., N_r$, and $\mathbf{n} \in \mathbb{C}^{N_r \times 1}$ is the received AWGN vector with entries n_j at the receiver input with zero mean and variance $\sigma_n^2 = N_o/2$ with N_o being the noise power spectral density. A RC MPAM signal has different intensity levels according to the symbol sequence as $(I_i^{\mathrm{PAM}} = \frac{\overline{I}}{M-1}(i-1),\ i = 1, 2, ..., M)$, where $\overline{I}$ denotes the average light intensity and M is the signal constellation size[13].

Channel state information (CSI) is considered available at the receiver side and maximum likelihood (ML) decoder is used to decode the received signals. The decoder decides the estimated active transmitter as[13]

$$\hat{k} = \arg\min_{k} \|\mathbf{r} - \eta \mathbf{H}\|_F^2, \tag{2}$$

where $\|.\|_F$ is the Frobenius norm[17].

For strong-turbulence condition, the channel irradiance h_{jk} can be modeled as an independent and identically distributed (IID) negative-exponential random variables (RVs) with probability density function (pdf) given by[3]

$$f_{h_{jk}}(h_{jk}) = \exp(-h_{jk}). \tag{3}$$

However, in moderate turbulence, h_{jk} can be modeled as an IID log-normal RV with pdf given by[4]

$$f_{h_{jk}}(h_{jk}) = \frac{1}{h_{jk}\sqrt{8\pi\sigma_x^2}} \times \exp\left(-\frac{(\ln(h_{jk}) - 2\mu_x)^2}{8\sigma_x^2}\right), \tag{4}$$

where $h_{jk} = \exp(2X_{jk})$ with X_{jk} being modeled as an IID Gaussian RV with mean μ_x and variance σ_x^2. To ensure that the fading channel does not attenuate or amplify the average power, the fading irradiances are normalized as $\mathbf{E}[h_{jk}] = e^{2(\mu_x + \sigma_x^2)} = 1$ (i.e., $\mu_x = -\sigma_x^2$).

A tight upper bound of the BER of SSK can be calculated by[13]

$$\mathrm{BER}_{\mathrm{SSK}}^{U} \leq \frac{1}{N_t \log_2(N_t)} \sum_{k=1}^{N_t} \sum_{i=1}^{N_t} d_H(b_k, b_i) \times Q\left(\frac{1}{N_r}\sqrt{\frac{\bar{\gamma}\log_2(N_t)}{2}\sum_{j=1}^{N_r}|h_{jk} - \hat{h}_{ji}|^2}\right), \tag{5}$$

where $Q(y) = \frac{1}{\sqrt{2\pi}}\int_y^{\infty} \exp(-\frac{x^2}{2})\mathrm{d}x$ is the Gaussian-Q function, with $\bar{\gamma} = (\eta\overline{I})^2/N_o$ being the average signal-to-noise ratio (SNR)[16]. The Hamming distance $d_H(b_k, b_i)$ counts the number of bit errors between received symbol, b_i, and transmitted symbol, b_k[11]. Besides, the $1/N_r$ term is added to make sure that the total area of the receivers is the same as the single-input single-output (SISO) receiver aperture[16] and $\hat{h}_{ji}$ is the channel irradiance between the receiver j and the estimated active transmitter i.

A tight lower bound of the BER of RC MPAM using maximum ratio combining (MRC) at the receiver is given by[18]

$$\mathrm{BER}_{\mathrm{RC}}^{L} \geq \frac{2(M-1)}{M\log_2(M)} \times Q\left(\frac{1}{N_r N_t (M-1)}\sqrt{\frac{\overline{\gamma}\log_2(M) N_r}{2}\sum_{j=1}^{N_r}\left(\sum_{k=1}^{N_t} h_{jk}\right)^2}\right). \tag{6}$$

The term $1/N_t$ is added to ensure that the total power for the N_t transmitters is the same as the active transmitter of SSK system[16] and the term $\sqrt{N_r}$ is due to the use of MRC where the noise variance in each aperture is equal to $N_o/2N_r$[16].

If X and Y are two independent RVs and $U = X - Y$, the pdf of U is equal to the cross correlation between the two pdfs as in Ref. [19, Eq. (4.160)]

$$f_U(u) = \int_{-\infty}^{\infty} f_X(u + y) f_Y(y)\mathrm{d}y. \tag{7}$$

Let $X \geq 0$ and $Y \geq 0$ be IID negative-exponential RVs, then it is shown in Ref. [17, Eq. (3.310)] that $f_U(u) = \exp(-|u|)/2$. If $Z = |U| = |h_{jk} - \hat{h}_{ji}|$ then $f_Z(z) = f_U(z) + f_U(-z) = \exp(-z)$. The histogram of the absolute difference of the two negative-exponential RVs and exact negative-exponential pdf are depicted in Fig. 2.

The pdf of the electrical SNR, $\gamma = z^2\bar{\gamma}$, can be obtained from the pdf of Z

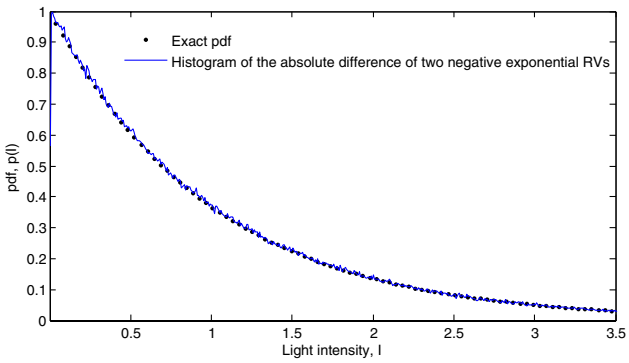

Fig. 2. Histogram of the absolute difference of the two negative-exponential RVs.

$$f_\gamma(\gamma) = \frac{1}{2\sqrt{\gamma\bar{\gamma}}}\ \exp\left(-\sqrt{\frac{\gamma}{\bar{\gamma}}}\right), \qquad \gamma > 0. \tag{8}$$

The MGF is defined by[20]

$$\Psi_\gamma(-s) = \int_0^\infty \exp(-s\gamma) f_\gamma(\gamma) \mathrm{d}\gamma. \tag{9}$$

Using Ref. [17, Eq. (3.322/2)], the MGF of Eq. (8) can be derived as

$$\Psi_\gamma(-s) = \sqrt{\frac{\pi}{s\bar{\gamma}}} \exp\left(\frac{1}{4s\bar{\gamma}}\right) Q\left(\sqrt{\frac{1}{2s\bar{\gamma}}}\right), \qquad s > 0. \tag{10}$$

Since the RVs are IID, the MGF of their difference becomes independent of the transmitter indices (i and k). Therefore, the Q function can be taken outside the summation in Eq. (5) and the 2-fold summation can be replaced by[21]

$$\frac{1}{N_t \log_2(N_t)} \sum_{k=1}^{N_t} \underbrace{\sum_{i=1}^{N_t} d_H(b_k, b_i)}_{N_t \log_2(N_t)/2} = \frac{N_t}{2}. \tag{11}$$

With the use of $Q(x) \approx \frac{1}{12}\mathrm{e}^{-\frac{x^2}{2}} + \frac{1}{4}\mathrm{e}^{-\frac{2x^2}{3}}$ which is accurate for $x > 0.5$[22] and Eq. (11), Eq. (5) can be rewritten as

$$\mathrm{BER}^U_{\mathrm{SSK}} \le \frac{N_t}{24}\ \exp\left(-\frac{\sum_{j=1}^{N_r} \gamma_j \log_2(N_t)}{4N_r^2}\right) + \frac{N_t}{8}\ \exp\left(-\frac{\sum_{j=1}^{N_r} \gamma_j \log_2(N_t)}{3N_r^2}\right). \tag{12}$$

The upper bound of the average BER (ABER) probability of SSK over negative-exponential channels can be obtained as, $\mathrm{ABER}^U_{\mathrm{SSK}} = \int_0^\infty \cdots \int_0^\infty \mathrm{BER}^U_{\mathrm{SSK}} f_\gamma(\gamma)\mathrm{d}\gamma$, where $\gamma = \gamma_1 \ldots \gamma_{N_r}$ and since the RVs are IID, the total MGF, $\Psi_T(-s) = \prod_{j=1}^{N_r} \Psi_{\gamma_j}(-s) = \Psi_\gamma(-s)^{N_r}$. The upper bound of the ABER using Eqs. (10)–(12) is derived as

$$\mathrm{ABER}^U_{\mathrm{SSK}} \le \frac{N_t \xi}{2}\left(\frac{1}{12}\Psi_\gamma\left(-\frac{\log_2(N_t)}{4N_r^2}\right)^{N_r} + \frac{1}{4}\Psi_\gamma\left(-\frac{\log_2(N_t)}{3N_r^2}\right)^{N_r}\right), \tag{13}$$

where ξ is added to improve the tight bound of the ABER of SSK over log-normal and negative-exponential channels. It is observed through extensive simulations and when employing different N_t and N_r that $\xi = 0.8$ will improve the tight bound for $N_r > 2$. SSK uses only an active transmitter at any time instance, so it cannot provide transmit diversity. Using Eq. (13) it is evident that the diversity gain of SSK is equal to N_r.

If X and Y are IID log-normal RVs, there exists no closed-form expression for the pdf of $Z = |X - Y|$, $f_Z(z)$. Hence, obtaining the ABER of SSK system over log-normal channel is analytically not possible. However, we assume that $f_Z(z)$ for moderate turbulence can be modeled approximately as G–G distribution. G–G channel represents the effective number of small-scale and large-scale eddies denoted by α and β, respectively[4]. To demonstrate the accuracy of this approximation, Fig. 3 shows a comparison between the exact and approximate pdf of the absolute difference of two log-normal RVs of $\sigma_x = 0.37$. In our work, extensive simulations are used to obtain accurate estimates of α and β. Figure 3 shows that G–G RVs with $\alpha = 3.3$ and $\beta = 1.1$ achieve accurate approximation.

The average lower bound BER probability of SSK over log-normal channels is shown to be equivalent to Eq. (13) with the MGF of G–G distribution using the series representation which was originally proposed by[23], $\Psi_I(-s)$, and after a few manipulations the MGF of the SNR of G–G[20] is given by

$$\Psi_\gamma(-s) = \sum_{p=0}^{\infty}\left[d_p(\beta,\alpha)\Gamma\left(\frac{\beta+p}{2}\right)(s\bar{\gamma})^{-\frac{\beta+p}{2}} + d_p(\alpha,\beta)\Gamma\left(\frac{\alpha+p}{2}\right)(s\bar{\gamma})^{-\frac{\alpha+p}{2}}\right], \tag{14}$$

where $\Gamma(w)$ is the gamma function defined as $\Gamma = \int_0^\infty t^{w-1} \exp(-t)\mathrm{d}t$ and $d_p(a,b)$ is given as

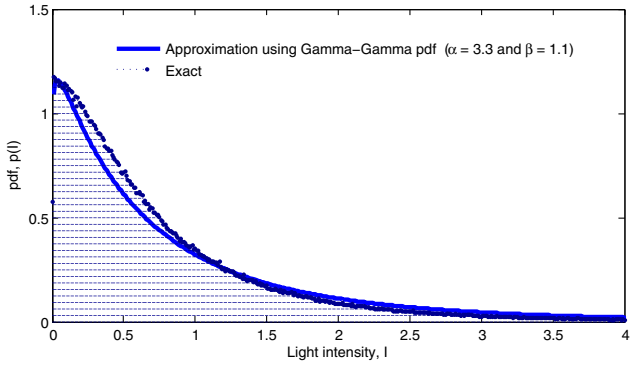

Fig. 3. Histogram of the absolute difference of two log-normal RVs ($\sigma_x = 0.37$ and $\mu_x = -\sigma_x^2$).

$$d_p(a,b) = \frac{\pi(ba)^{a+p}}{2\sin[\pi(b-a)]p!\Gamma(b)\Gamma(a)\Gamma(a-b+p+1)}. \quad (15)$$

In the analysis, the ABER performance of SSK and RC MPAM are compared with respect to that of SNR. Different scenarios over negative-exponential or log-normal channels are employed while considering similar spectral efficiency for compared systems. Hence, MPAM and SSK provide spectral efficiency of $\log_2(M)$ and $\log_2(N_t)$ bits/s/Hz, respectively. It is shown that the upper bound in Eq. (5) is loose at low SNR values but tightens at pragmatic values. This is in accordance with other obtained results using similar bound as in Refs. [13,18]. For negative-exponential, it is worth mentioning that the ABER of SISO is considered as a benchmark using Eq. (6) with $N_t = N_r = 1$ as in Ref. [7]. For log-normal channels, the ABER of SISO is considered as in Ref. [24], while using MPAM for fair comparison with the same spectral efficiency of Figs. 4–6.

Furthermore, the performance of commercially available MIMO systems using RCs with $N_t = N_r = 2$ and employing OOK modulation is compared with that of the proposed SSK system. For this purpose and for the sake of fair comparison, the power of OOK ($\bar{\gamma}$ is proportional to the square of the IM/DD optical power) is normalized by $\log_2(M)$.

To achieve a spectral efficiency of 3 bits/s/Hz, an 8×8 MIMO system is considered and the simulation results are reported in Fig. 4. Analytical and simulation results show close match for a wide range of SNR values which support the analysis. Additionally, Fig. 4 shows that SSK outperforms RC system for SNR <28 dB. This is due to the benefits of SSK over RC MPAM, namely, increased SNR gain along with greater spectral efficiency and/or higher turbulence effects. This, while RC systems show better performance at higher SNR due to the high diversity gain. Increasing the number of receivers to ten instead of eight enhances the performance of SSK systems as compared to RC for high SNR. The SSK system gains about 2 dB in SNR at ABER of 10^{-6}.

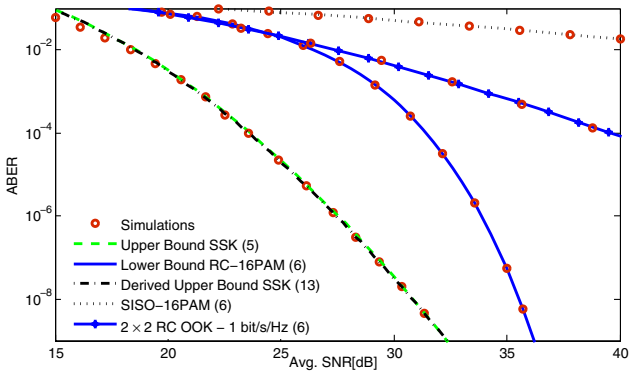

Fig. 5. Comparison of SSK and RCs with spectral efficiency = 4 bits/s/Hz in a negative-exponential channel with $N_t = 16$ and $N_r = 16$.

Figure 5 shows the results of increasing the spectral efficiency to 4 bits/s/Hz. This increase is made by considering a 16×16 MIMO setup. SSK system shows superior performance as compared to RC and a gain of about 6.5 dB is achieved at ABER of 10^{-6}. Simulation results in Fig. 5 depict the case of an ABER of 10^{-9} and shows the accuracy of the Q-function approximation[25].

Finally, Fig. 6 shows the case of a moderate turbulence in a log-normal channel with $\sigma_x = 0.37$ as an example of a moderate turbulence. Based on the approximation, the results of which are shown in Fig. 3, the MGF of G–G is used to derive a tight bound ABER for SSK over log-normal channel. This approximation leads to a narrow gap between the upper bound Eq. (5) and the derived lower bound of SSK. This is unlike the results shown in Figs. 4 and 5, which are based on exact MGF of the absolute difference of negative-exponential RVs. Obtained results show that at an ABER of 10^{-6}, SSK gains 4 and 7.5 dB over RC 16-PAM and RC OOK (2×2), respectively. The SNR corresponding to RC illustrated in Fig. 6 is lower than that of the RC illustrated in Fig. 5 by 0.3 dB,

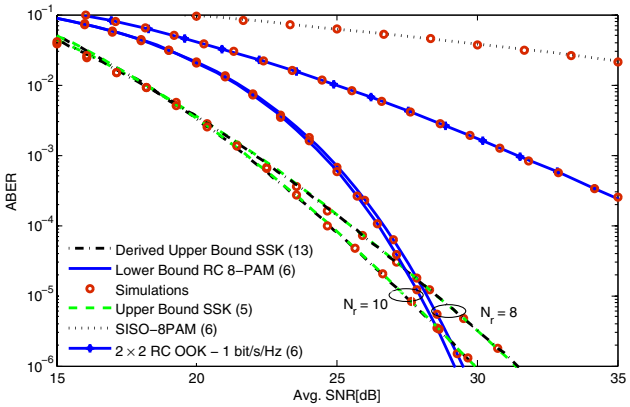

Fig. 4. Comparison of SSK and RCs with spectral efficiency = 3 bits/s/Hz in a negative-exponential channel with $N_t = 8$ and increasing the number of receivers $N_r = 8$ and 10.

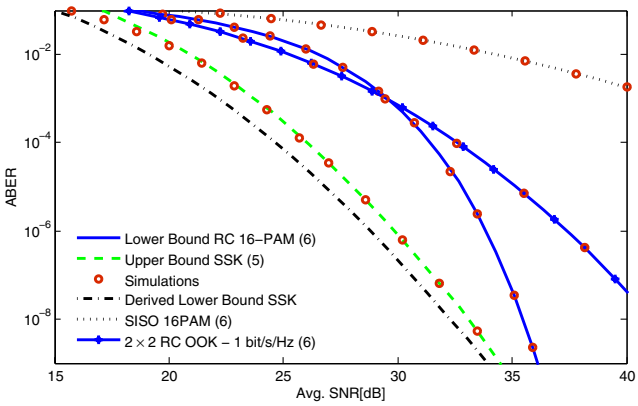

Fig. 6. Comparison of SSK and RCs with spectral efficiency = 4 bits/s/Hz in a log-normal channel with $\sigma_x = 0.37$, $N_t = 16$ and $N_r = 16$.

while SSK system is shown to perform better in strong turbulent channels as compared to moderately turbulent channels. This is mainly because the ABER of SSK system is not determined by the actual channel realizations as in the case of RCs and SISO, rather by the differences among different channels associated with various transmitters.

It is shown that the SSK system outperforms RC MPAM system for large number of transmitters, however, it might not be feasible in all applications, since the SSK uses a single transmitter at each time instant and all others are off for that time. Hence, single-stream transmitter are needed and the active transmit unit, among the spatially separated units, is selected each time instant based on the incoming bits sequence. As such, transmitter synchronization requirement is omitted and complexity is significantly reduced enabling the use of large number of transmitters.

In conclusion, the ABER performance of FSO links with SSK over negative-exponential and log-normal atmospheric turbulence channels are investigated. Tight upper and lower bounds for ABER expressions corresponding to negative-exponential channels and log-normal channels, respectively, are obtained. In comparison to SISO and RC MPAM techniques, our results are in favor of SSK FSO links for high-spectral-efficiency applications and/or channel high-turbulence effects. Moreover, increasing the number of receivers is shown to yield lower SNR in SSK systems as compared to RC MPAM systems.

References

1. M. A. Khalighi and M. Uysal, IEEE Commun. Surv. Tut. **16**, 2231 (2014).
2. C. Tang, R. Li, Y. Shao, N. Chi, J. Yu, Z. Dong, and G. K. Chang, Chin. Opt. Lett. **11**, 020608 (2013).
3. W. O. Popoola and Z. Ghassemlooy, J. Lightw. Technol. **27**, 967 (2009).
4. A. A. Farid and S. Hranilovic, J. Lightw. Technol. **25**, 1702 (2007).
5. M. Abaza, R. Mesleh, A. Mansour, and E.-H. M. Aggoune, SPIE Opt. Eng. **53**, 1 (2014).
6. B. Epple, IEEE/OSA J. Opt. Commun. Netw. **2**, 293 (2010).
7. H. E. Nistazakis, V. D. Assimakopoulos, and G. S. Tombras, Optik **122**, 2191 (2011).
8. K. Sripimanwat, J. Wongpoom, and O. Sangaroon, Chin. Opt. Lett. **11**, 100602 (2013).
9. Y. Wang and N. Chi, Chin. Opt. Lett. **12**, 100603 (2014).
10. R. Mesleh, H. Haas, S. Sinanović, C. W. Ahn, and S. Yun, IEEE Trans. Veh. Technol. **57**, 2228 (2008).
11. R. Mesleh, R. Mehmood, H. Elgala, and H. Haas, in *Proceedings of IEEE International Conference on Communications* 1 (IEEE, 2010).
12. M. D. Renzo, H. Haas, A. Ghrayeb, S. Sugiura, and L. Hanzo, Proc. IEEE **102**, 56 (2014).
13. T. Fath, H. Haas, M. Di Renzo, and R. Mesleh, in *Proceedings of IEEE Global Communications Conference* 1 (IEEE, 2011).
14. T. Ozbilgin and M. Koca, in *Proceedings of IEEE International Conference on Communications* 3412 (IEEE, 2014).
15. G. Yang, M.-A. Khalighi, T. Virieu, S. Bourennane, and Z. Ghassemlooy, in *Proceedings of IEEE International Workshop on Optical Wireless Communications* 1 (IEEE, 2012).
16. T. A. Tsiftsis, H. G. Sandalidis, G. K. Karagiannidis, and M. Uysal, IEEE Trans. Wireless Commun. **8**, 951 (2009).
17. I. S. Gradshteyn and I. M. Ryzhik, *Table of Integrals, Series, and Products* (Academic, 2007).
18. T. Fath and H. Haas, IEEE Trans. Commun. **61**, 733 (2013).
19. J. J. Shynk, *Probability, Random Variables, and Random Processes: Theory and Signal Processing Applications* (Wiley, 2012).
20. M. Aggarwal, P. Garg, P. Puri, and P. K. Sharma, in *Proceedings of IEEE International Conference on Signal Processing and Integrated Networks* 333 (IEEE, 2014).
21. M. D. Renzo and H. Haas, IEEE Trans. Veh. Technol. **61**, 1124 (2012).
22. M. Chiani, D. Dardari, and M. K. Simon, IEEE Trans. Wireless Commun. **2**, 840 (2003).
23. E. Bayaki, R. Schober, and R. K. Mallik, IEEE Trans. Commun. **57**, 3415 (2009).
24. S. M. Navidpour, M. Uysal, and M. Kavehrad, IEEE Trans. Wireless Commun. **6**, 2813 (2007).
25. Q. Zhang, J. Cheng, and G. K. Karagiannidis, IET Commun. **8**, 616 (2014).